PHASE FORMATION, MICROSTRUCTURE AND FUNCTIONAL PROPERTIES OF SOME $BaTi_{1-X}Zr_XO_3$ CERAMICS

Cătălina A. VASILESCU[1], Lavinia P. CURECHERIU[2], Liliana MITOŞERIU[3], Adelina C. IANCULESCU[4*]

$BaTi_{1-x}Zr_xO_3$ ($0 \leq x \leq 0.20$) solid solutions were prepared by solid state reaction method. XRD investigations showed the formation of individual $BaTiO_3$ss (solid solution) and $BaZrO_3$ss perovskite phases, from the ceramic samples with higher Zr content ($x \geq 0.10$). All the ceramics under investigation were single-phased after sintering at 1500°C for 4 hours. Dielectric measurements indicated a maximum of permittivity only for the sample corresponding to undoped $BaTiO_3$. All Zr-doped ceramic samples showed diffuse phase transition. The increase of the solute content induces the decrease of the ferroelectric – paraelectric phase transition temperature. The diffuseness corresponding to the permittivity maxima originates not only in the increase of Zr content, but also in some particular microstructural features.

Keywords: Dielectric properties, ferroelectric – paraelectric phase transition

1. Introduction

Ferroelectric materials are used in many modern technologies such as piezoelectric actuators and electro-optic modulators. One of the most extensively studied perovskite (ABO_3 structure), ferroelectric oxide, is barium titanate ($BaTiO_3$). Given to its excellent dielectric and ferroelectric properties it is exploited in various electronic devices as multi layer ceramic capacitors – MLCC, pyroelectric detectors, thermistors, PYCR sensors, transducers, controller, pulse generating devices, and nonvolatile memories in microelectronic industry [1-6]. The properties of barium titanate ceramics are strongly dependent on parameters like: grain size, density, impurities and structural defects. Barium titanate doped with Zr [7], Hf [8], Ce [9], Y [10] and Sn [11] shows relaxor behavior with improved dielectric performances, very high permittivity, piezoelectric and pyroelectric constants and the lack of macroscopic hysteresis $P(E)$ loop, as well.

[1] Science and Engineering of Oxide Materials and Nanomaterials, University POLITEHNICA of Bucharest, Romania, e-mail: katyvasilescu85@yahoo.com
[2] Department of Physics, "Al. I. Cuza" University, Bv. Carol 11, 700506, Iasi, Romania
[3] Department of Physics, "Al. I. Cuza" University, Bv. Carol 11, 700506, Iasi, Romania
[4] Science and Engineering of Oxide Materials and Nanomaterials, University POLITEHNICA of Bucharest, Romania, a_ianculescu@yahoo.com

Alternatively, $BaTiO_3$-based solid solutions are environment-friendly dielectrics with performances which tend to be similar to those of many Pb-based electroceramics.

By *B*-site doping in the ABO_3 perovskite lattice of barium titanate, the cooperative dipolar long-range order formed by the off-center displacement of Ti^{4+} ions in their TiO_6 octahedra is disrupted. This often leads to a broadening of the transition in the range of Curie temperature, inducing the so-called *diffuse phase transition*. From this point of view, zirconium is well known as one of the most effective solutes in $BaTiO_3$ [12]. Zr^{4+} ion has a larger ionic radius (0.72 Å) than that one of Ti^{4+} (0.605 Å); it induces the expansion of the perovskite lattice. In $Ba(Ti_{1-x}Zr_x)O_3$ (BTZ) system, Zr/Ti ratio is a very important parameter which tailors the type of the ferroelectric – paraelectric phase transition and its characteristic Curie temperature. Thus, it was found that BTZ bulk ceramic exhibits a pinched phase transition at $x = 0.15$, where all the three dielectric constant peaks coalesce into a single broad maximum [7, 13]. Moreover, Zr^{4+} ion is chemically more stable than the host Ti^{4+} or other *B*-site solutes, as tin or cerium, which are more versatile, due to their multiple valence state. Consequently, replacing Ti by Zr would depress the conduction by small polarons hopping between Ti^{4+} and Ti^{3+}, and it would also decrease the leakage current. This makes the barium titanate zirconate $Ba(Ti, Zr)O_3$ (BTZ) a promising candidate as an alternative material to barium strontium titanate $(Ba, Sr)TiO_3$ in dynamic random access memories (DRAM), non-volatile random access memories (NVRAM), and other microwave applications.

Despite the assiduous research that has been carried out over the years and the numerous data published in literature [14-18], the dielectric behavior of $BaTi_{1-x}Zr_xO_3$ (BTZ) solid solutions remains a controversial matter. Even for ceramic materials obtained via the traditional solid-state reaction route, different values of dielectric properties, Curie temperature and morphotropic composition were reported. Dissimilar features of the ferroelectric – paraelectric phase transition were also found for compositions with the same Zr content. This spread of the experimental results may be explained in terms of dissimilar microstructures induced by the different processing parameters used in various studies. Generally, the microstructural features of BTZ ceramics and their influence on the functional properties were less investigated and some results were reported only in the last few years [19]. The aim of this work was to study the mechanism of phase formation and the microstructure and dielectric behaviour of some $BaTi_{1-x}Zr_xO_3$ ($0 \le x \le 0.20$) ceramics prepared by the solid-state reaction method.

2. Experimental procedure

$BaTi_{1-x}Zr_xO_3$ solid solutions (x = 0; 0.05; 0.10; 0.15; 0.20) have been prepared by classical ceramic method from p.a. grade oxides and carbonates: TiO_2 (Merck), ZrO_2 (Merck) and $BaCO_3$ (Fluka), by wet homogenization technique in iso-propanol.

The initial mixtures were dried at room temperature and shaped by uniaxial pressing at 160 MPa into pellets of 20 mm diameter and ~ 3 mm thickness. After the presintering thermal treatment performed in air at 1200°C for 3 hours, the samples were finely grounded in an agate mortar, pressed again into pellets (of 13 mm diameter and ~ 2 mm thickness), using an organic binder (polyvinyl alcohol – PVA). These pellets were sintered in air at 1500°C, with a heating rate of 5°C/min, and a soaking time of 4 hours, and then they were slowly cooled at normal cooling rate of the furnace.

The processes which take place during the heating of the mixtures of raw materials were monitored by means of thermal analysis methods, as Differential Scanning Calorimetry (DSC) and Differential Thermal Gravimetry (DTG), using a Netzsch STA 409 PC Luxx thermal analyzer. These investigations were carried out in static air atmosphere up to 1200^oC, with a heating rate of 10 $K \cdot min^{-1}$.

X-ray diffraction measurements at room temperature used to investigate the purity of the perovskite phases were performed with a SHIMADZU XRD 6000 diffractometer, using Ni-filtered CuKα radiation (λ = 1.5418 Å) with a scan step increment of 0.02° and with a counting time of 1 s/step, for 2θ ranged between 20 – 80°.

A HITACHI S2600N scanning electron microscope coupled with EDX was used to analyse the microstructure and to check the chemical composition of the ceramic samples.

The electrical measurements were performed on parallel-plate capacitor configuration, by applying Pd - Ag electrodes on the polished surfaces of the sintered ceramic disks. The complex impedance in the frequency range of (1 – 10^6) Hz was determined by using an impedance analyzer (Solartron, SI 1260). For low temperatures, the complex impedance in the frequency domain (1-10^6 Hz) was determined by using a dielectric spectrometer CONCEPT 40 Novocontrol Tehnologies. The measurements at high voltages were performed by placing the electrode ceramic pellets in a cell containing transformer oil. For obtaining accurate tunability data, a circuit was designed and realized [22], in which the high voltage was obtained from a function generator coupled with a TREK 30/20A-H-CE amplifier.

3. Results and discussions

3.1. Phase formation

Thermal analysis data for mixtures 1 ($x = 0$) and 4 ($x = 0.15$) were found to be very similar and they are presented in Figs. 1(a) and (b).

The occurrence of an endothermic peak on the DSC curve at 808°C was attributed to the polymorphic transformation of $BaCO_3$. The endothermic peak that can be noticed at 930°C is due to the decarbonation process with the formation of the perovskite structure.

Above 950°C, the heat capacity of the sample varies suddenly, and the DSC curves record an ascendant slope which effectively hides all subsequent, higher temperature decarbonation stages. However, the small endothermic peaks recorded on the DTG curves at temperatures of around 1015°C bring forward the existence of these effects.

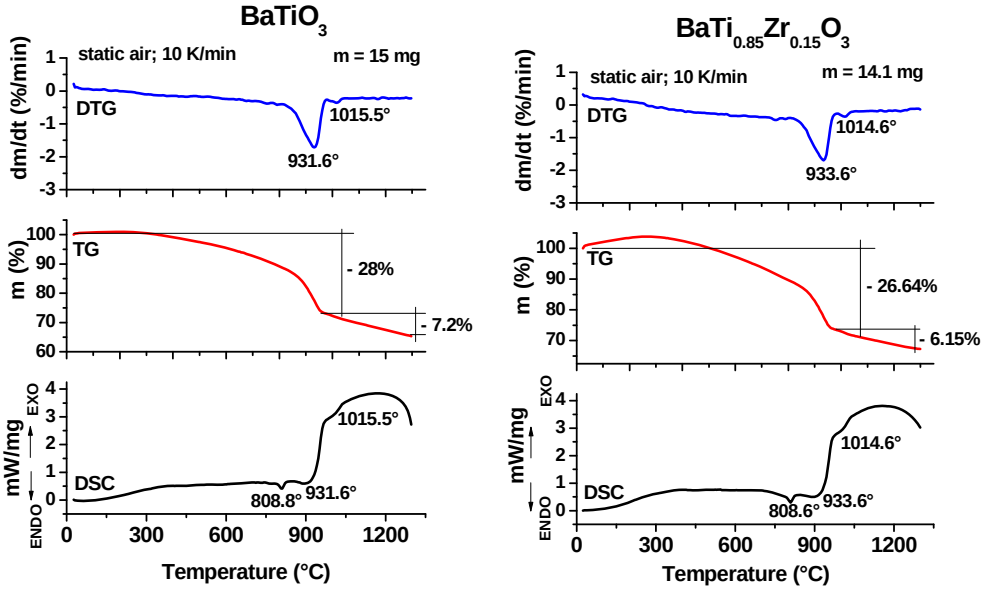

Fig. 1. Thermal analysis curves for the mixtures: (a) 1 ($x = 0$) and 5 (x = 0.15).

XRD investigations carried out on the ceramic samples thermally treated at 1200°C and slowly cooled at room temperature, indicated that only the undoped $BaTiO_3$ sample was single phased (eq. 1). For the Zr-doped ceramics, beside the major perovskite phase, some amounts of un-reacted raw materials (TiO_2 and ZrO_2) and non-equilibrium compounds (Ba_2TiO_4) (eq. 2), more or less significant from quantitative point of view depending on the starting Zr concentration, were

detected as secondary phases (Fig. 2(a)). The increase of thermal treatment temperature induces the evolution of the interaction processes (eq. (3)), so that the samples with lower Zr content (x = 0.005 and 0.10) became single-phased. For the ceramics with higher solute concentrations (x = 0.15 and 0.20) two distinct perovskites, the first one corresponding to $BaTiO_3$ solid solution and the second with the structure of $BaZrO_3$, were identified as major and minor phases, respectively (Fig. 2(b)). This secondary $BaZrO_3$ phase ($BaZrO_3$ss) can be visualized as small asymmetrical features located at the left side of the profiles of the main diffraction peaks specific to the major $BaTiO_3$ss phase in the diffraction patterns of Fig. 2(b). This evolution indicates a two-step process, consisting of a clear tendency of individual formation of the two limit compounds $BaTiO_3$ and $BaZrO_3$ at lower temperatures (eq. 4), followed by the high temperature formation of the solid solutions corresponding to the nominal formulae (eq. 5)). This last process takes place by inter-diffusion phenomena, implying the incorporation of Zr^{4+} into $BaTiO_3$ lattice, concurrently with the integration Ti^{4+} onto Zr^{4+} sites in $BaZrO_3$ lattice. The higher the content of zirconium in the starting mixture, the higher will be the temperature at which a single-phase BTZ solid solution is formed. The XRD patterns of Fig. 2(c) show that all the investigated ceramics are monophasic after sintering at 1500^oC for 4 hours. The formation mechanism of BTZ solid solutions is described by the reactions (1) – (5).

$$BaCO_3 + TiO_2 \rightarrow BaTiO_3 \quad (1)$$

$$2BaCO_3 + TiO_2 \rightarrow Ba_2TiO_4 \quad (2)$$

$$Ba_2TiO_4 + TiO_2 \rightarrow 2BaTiO_3 \quad (3)$$

$$BaCO_3 + ZrO_2 \rightarrow BaZrO_3 \quad (4)$$

$$(1-x)BaTiO_3 + x\ BaZrO_3 \rightarrow BaTi_{1-x}Zr_xO_3 \quad (5)$$

The quantitative incorporation of Zr^{4+} on Ti sites into $BaTiO_3$ lattice for all the investigated ceramic samples is proved by the gradual shift of the main diffraction peaks towards lower values of the diffraction angle, which is specific to the *B*-site doping with species of higher ionic radius (Fig. 2(c)).

The evolution of the unit cell symmetry of the BTZ solid solutions against Zr content was qualitatively estimated by the change of the profile corresponding to the (002)/(200) diffraction peak, which is the most sensitive to the structural modifications. Thus, the detail of the diffraction pattern (orange rectangle of Fig. 2(c)), corresponding to the 2θ range of 44.5 – 46^o, shows that the split (002)/(200) peak, indicating a tetragonal distortion specific to the un-doped $BaTiO_3$, gradually merged into a single (200) peak, specific to the cubic symmetry, in the case of the highly Zr-doped ceramics (Fig. 2(d)).

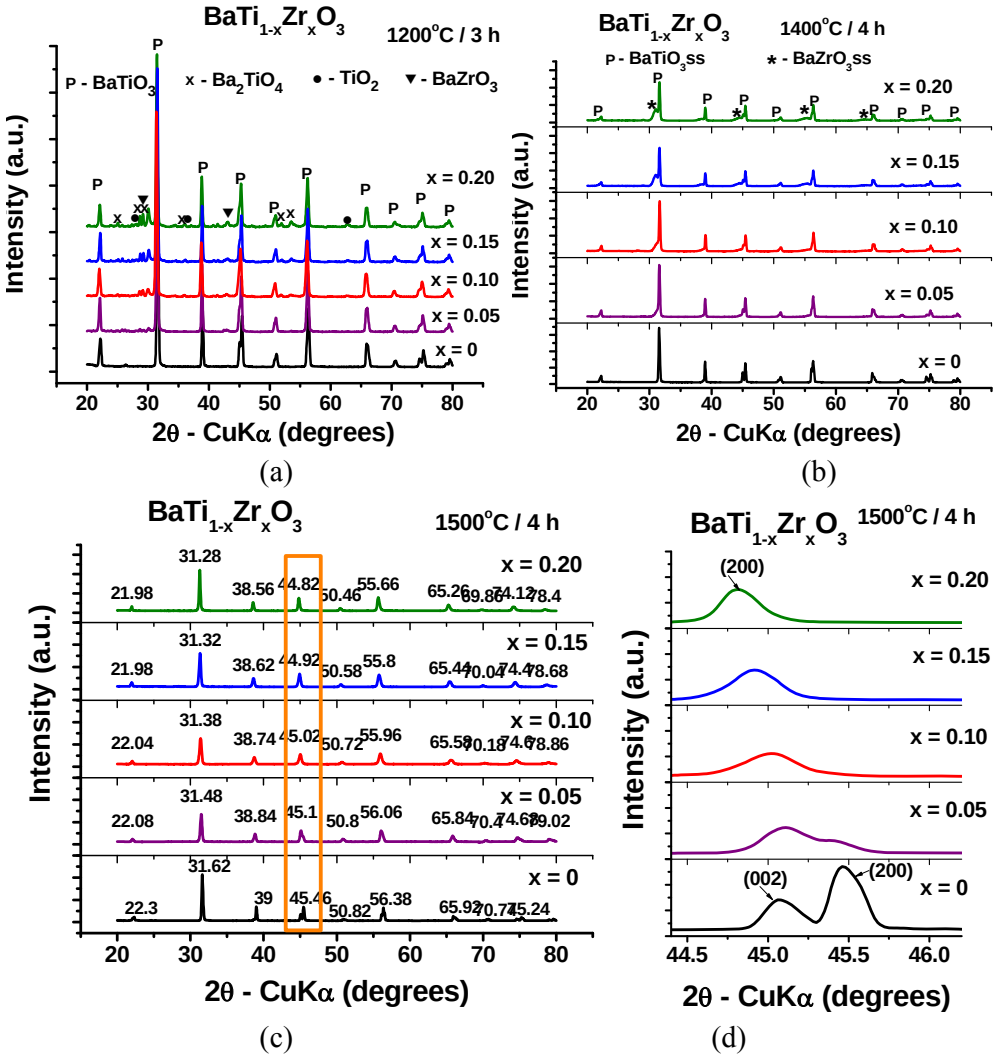

Fig. 2. Room temperature XRD patterns of the $BaTi_{1-x}Zr_xO_3$ ceramic samples obtained after thermal treatment at: (a) 1200°C / 3 hours; (b) 1400°C / 4 hours; (c) 1500°C / 4 hours and (d) detail of the diffraction pattern (orange rectangle of Fig. 3(c)), corresponding to the 2θ range of 44.5 – 46°, showing the evolution of the profile of the (002)/(200) diffraction peak

3.2. Microstructure

The microstructure of the ceramics strongly depends on the solute concentration. An obvious decreasing tendency of both the average grain size and density was noticed when the Zr content increases. Thus, while the undoped, highly densified $BaTiO_3$ ceramic bulk sample exhibits large, irregular grains (of ~ 136 μm), with well-defined grain boundaries and almost perfect triple junctions

(Figs. 3(a),(b)), in the case of Zr-doped ceramics, SEM images indicate a drastic disturbance of the microstructure, which becomes more porous and more fine-grained, as the Zr content increases (Figs. 3(c)-(f)). Thus, significantly smaller grains (of ~ 6 μm) with not well-defined shape were noticed for the BTZ ceramics with x = 0.15 and x = 0.20, respectively. It is believed that the microstructural refinement accompanied by the increase of the intergranular porosity inducing a poor densification in highly Zr-doped barium titanate ceramics originates most likely in the so-called Kirkendall effect caused by the different diffusion rates of the cationic species that compose the BZT solid solutions [20].

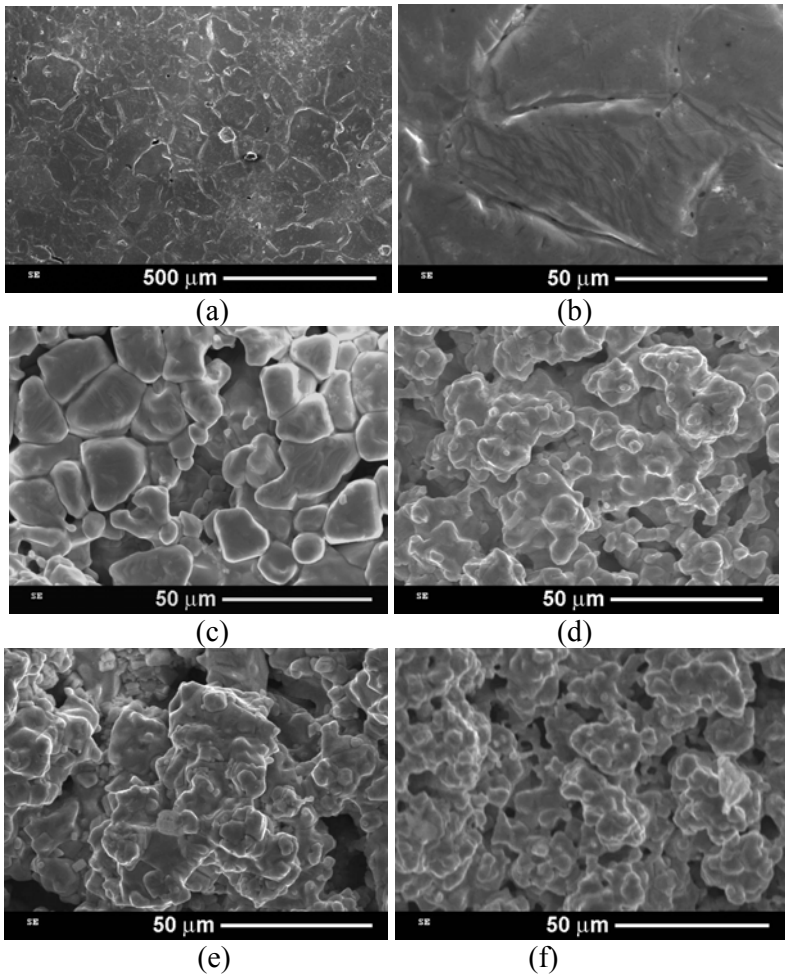

(a) (b) (c) (d) (e) (f)

Fig. 3. SEM images of $BaTi_{1-x}Zr_xO_3$ ceramics sintered at 1500°C / 4 hours: (a), (b) x = 0 ((a) general view; (b) detail); (c) x = 0.05; (d) x = 0.10; (e) x = 0.15 and (f) x = 0.20.

3.3. Dielectric properties

Fig. 4(a) shows that the increase of the Zr content causes a gradual shift o the ferroelectric – paraelectric phase transition temperature towards lower temperature values, so that for the composition with x = 0.20 this phase transition occurs in the proximity of the room temperature. Moreover, the increase of the Zr addition also contributes to the change of the type of phase transition, from a displacive one (a first order phase transition), specific to pure $BaTiO_3$, to a transition of second order (order-disorder transition), characteristic for the ceramics with higher Zr concentration ($x \geq 0.15$). One can see that only the undoped sample show a sharp permittivity maximum, whereas the Zr-doped ceramics exhibit larger and more flattened (more "diffuse") $\varepsilon(T)$ maxima, as the Zr addition increased. It is generally accepted that the modification of the type of phase transition reflected in the flattening of the dielectric maximum with the increase of *B*-site doping originates from internal microstrains generated in the perovskite lattice because of radii mismatch between Zr and Ti cations, or because of local chemical inhomogeneities [18, 19]. However, it is worthy to mention that the diffuseness of the phase transition is not gouverned only by the dopant addition, but also by specific microstructural features, mainly by the grain size. Thereby, the lower the average grain size, the more "diffuse" becomes the ferroelectric – paraelectric phase transition [19].

A method to emphasize the increasing relaxor character when increasing the Zr addition, *x*, is to use the empirical formula derived from the Curie-Weiss law, as proposed in the ref. [21] and often used for other $BaTiO_3$-based solid solutions [22, 23] or for Pb-based relaxors [24]:

$$\varepsilon = \frac{\varepsilon_m}{1+\left(\frac{T-T_m}{\delta}\right)^{\eta}} \tag{6}$$

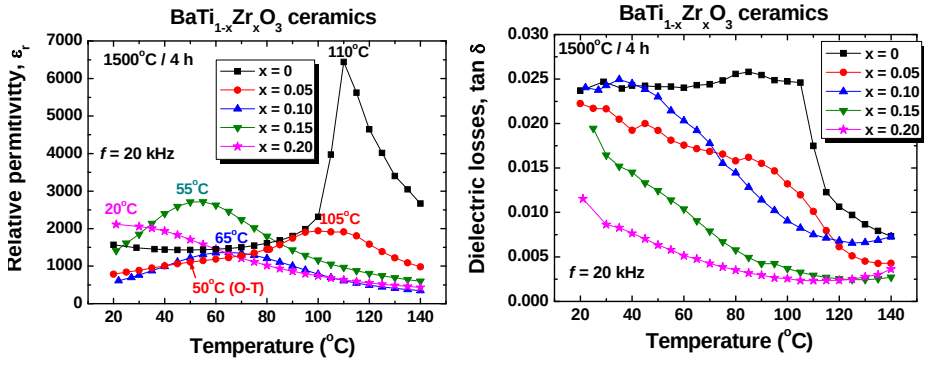

(a) (b)

Fig. 4. Dielectric properties of $BaTi_{1-x}Zr_xO_3$ ceramics sintered at 1500°C for 4 hours: (a) dielectric permittivity; (b) dielectric losses

This equation, with unique values of parameters η and δ for all the frequencies, describes the dielectric properties of relaxors, even in the dielectric dispersion region [25, 26]. The parameter η gives information on the character of the phase transition: for $\eta = 1$, normal Curie-Weiss law is obtained, while $\eta = 2$ describe a complete diffuse phase transition specific to a relaxor state. In the latter case, δ has the dimension of a temperature and indicates the range of temperature extension for the diffuse phase transition, owing to the direct correlation with the dielectric permittivity broadening. For a ferroelectric material, eq. (6) reduces to the Curie-Weiss law with $\eta = 1$ and in this situation δ is proportional to the Curie constant. Table 1 shows the values of these parameters for the studied ceramics, as resulted from the linear fit of the dielectric data according to the eq. (6). The evolution towards the relaxor state with increasing x is demonstrated by the increasing of the both empirical paramateres η (which increases from 1.00, for x = 0, to 1.95, for x = 0.20) and of the temperature extension of the diffuse phase transition δ (which increases from 21.5, for x = 0.05, to 59.16, for x = 0.20). It is interesting to point out that even the BTZ composition with x = 0.05 shows unexpectedly high values of these parameters, which proves that even for a lower solute content, a significantly lower average grain size (of 13.2 μm in this case) can induce diffuse ferroelectric – parelectric phase transitions. The values of the mentioned parameters obtained in this study for our BTZ ceramics, are somewhat higher than those reported in the literature for ceramics with similar compositions, also prepared via solid state reaction method [12, 13]. Thus, Hennings *et al*. [13] obtained a very sharp permittivity maximum for their BTZ sample with x = 0.13. The η and δ values in our case, are also higher than the values corresponding to $BaTi_{1-x}Sn_xO_3$ ceramics with similar solute contents, also prepared via solid state reaction method and sintered at a lower temperature (1300°C for 4 hours) [27]. The highest value of the dielectric constant (of 7138) was obtained for pure $BaTiO_3$ at a Curie temperature of 110°C (Table 1), somewhat lower than the Curie temperature values of 120 – 135°C, usually reported for pure $BaTiO_3$.

Table 1

Dielectric parameters of $BaTi_{1-x}Zr_xO_3$ ceramics sintered at 1500°C for 4 hours

x	ε_m	T_m (°C)	η	δ (°C)
0	7138	110	1	21.5
0.05	1942	100	1.21	31.64
0.10	1381	65	1.34	40.29
0.15	2784	55	1.52	37.60
0.20	2112	20	1.95	59.16

The orthorhombic – tetragonal phase transition can be observed in Fig. 4(a) only for the lower Zr contents, *i.e.* for the BTZ sample with x = 0.05 and it occurs at 50°C. For the undoped $BaTiO_3$ ceramic it is most likely that this phase

transition takes place at a temperature below the measuring range. For higher Zr concentrations all the phase transitions merge into a single one which occurs at a temperature value denoted T_m. The coalescence of the three permittivity peaks corresponding to the phase transitions of pure $BaTiO_3$, into a unique, large peak is specific to homovalently *B*-site doped $BaTiO_3$ and was widely reported in the literature [13], [15-16].

Regarding the dielectric loss, there were found low values ($\tan \delta < 0.03$) for all the ceramic samples under investigation (Fig. 4(b)). The lowest dielectric losses were recorded for the ceramic with x = 0.20, almost over all the temperature range in which dielectric measurements were performed.

4. Conclusions

$BaTi_{1-x}Zr_xO_3$ ($0 \leq x \leq 0.20$) solid solutions were prepared by the solid state reaction method. For the ceramic samples with higher Zr content ($x \geq 0.10$), XRD investigations showed the formation of individual $BaTiO_3$ss and $BaZrO_3$ss perovskite phases. All the ceramics under investigation were single-phased after sintering at 1500^{o}C / 4 hours.

The crystalline structure and microstructure of BTZ ceramics strongly depended on the Zr content. The addition of Zr induced a drastic decrease of the average grain size from 136 μm, for undoped $BaTiO_3$, to 13.2 μm, for the composition with x = 0.10, and to ~ 6 μm for the ceramics with x = 0.15 and 0.20. The microstructural refinement is accompanied by the subsequent increase of the intergranular porosity by Kirkendall effect.

Dielectric measurements indicated sharp permittivity maximum only for the sample corresponding to undoped $BaTiO_3$. All the Zr-doped ceramic samples showed diffuse phase transition. The increase of the solute content induces the decrease of the ferroelectric – paraelectric phase transition temperature. The diffuseness corresponding to the permittivity maxima originates not only in the increase of Zr content, but also in some particular microstructural features.

Acknowledgement

The first author acknowledges the financial support of the Romanian CNCS-UEFISCDI Project No. PN-II-ID-PCE-2011-3-0668 and POSDRU/107/1.5/S/76813. This work has also been performed in the frame of 7.15 theme of the Romanian Academy program: “Oxide systems obtained by the sol-gel method” (2012).

REFERENCES

[1] *A. Rae, M. Chu, V. Ganine*, Barium titanate – Past, present and future, pp. 1–12 in Ceram. Trans. 2007, vol. **100**, Dielectric Ceramic Materials, Ed. by K.M. Nair, A.S. Bhalla, The American Ceramic Society, Westerville, OH, 1999.

[2] *X. Ren*, Large electric-field-induced strain in ferroelectric crystals by point-defect-mediated reversible domain switching, Nat. Mater. **3**, (2004), 91-94.

[3] *M. E. Lines, A. M. Glass*, Principles and applications of ferroelectrics and related materials, Clarendon, Oxford, 1977.

[4] *G. H. Haertling*, Ferroelectric Ceramics: History and Technology, J. Am. Ceram. Soc. **82**, (1999), 797-818.

[5] *J. M. Wilson*, Minerals Review – Barium titanate, Am. Ceram. Soc. Bull. 74, (1995), 106-110.

[6] *J. S. Capurso, A.A. Bologna, W.A. Schulze*, Processing of laminated $BaTiO_3$ structures for stress-sensing applications, J. Am. Ceram. Soc. **78**, (1995), 2476-2480.

[7] *Z. Yu, C. Ang, R. Guo,A. S. Bhalla*, Piezoelectric and strain properties of $Ba(Ti_{1-x}Zr_x)O_3$ ceramics, J. Appl. Phys. **92**, (2002), 2655-2657.

[8] *W. H. Payne and V. J. Tennery*, Dielectric and Structural Investigations of the. System $BaTiO_3$-$BaHfO_3$, J. Am. Ceram. Soc. **48**, (1965), 413-417.

[9] *A. Chen, Y. Zhi, J. Zhi, P. M. Vilarinho, J. L. Baptistam*, Synthesis and characterization of Ba $(Ti_{1-x}Ce_x)O_3$ ceramics, J. Eur. Ceram. Soc. **17**, (1997), 1217-21.

[10] *J. Zhi, A. Chen, Y. Zhi, P. M. Vilarinho and J. L. Baptista*, Dielectric properties $Ba(Ti_{1-y}Y_y)O_3$ ceramics, J. Appl. Phys. **84**, (1998) 983-986.

[11] *X. Wei, Y.J. Feng, and X. Yao*, Dielectric relaxation behavior in barium stannate ferroelectric ceramics with diffused phase transition, Appl. Phys. Lett. **83**, (2003), 2031-2033.

[12] *R.C Kell, N.J Hellicar*, Structural Transitions in Barium Titanate-Zirconate Transducer Materials, Acustica, **6** (1956) 235-238.

[13] *D. Hennings, A. Schnell, G. Simon*, Diffuse Ferroelectric Phase Transitions in $Ba(Ti_{1-y}Zr_y)O_3$ Ceramics, J. Am. Ceram. Soc. **65**, (1982), 539-544.

[14] *T. N. Verbitskaya, G. S. Zhdanov, Y. N. Venevtsev, S. P. Solov'ev*, Electrical and X-Ray diffraction studies of the $BaTiO_3$-$BaZrO_3$ system, Sov. Phys. – Crystallogr. (Engl Transl*)* **3**, (1958), 182-92.

[15] *T. Maiti, R. Gu, A. S. Bhalla*, Structure-property phase diagram of $BaZr_xTi_{1-x}O_3$ system, J. Am. Ceram. Soc. **91**, (2008), 1769-80.

[16] *A. Simon, J. Ravez, M. Maglione*, The crossover from a ferroelectric to a relaxor state in lead-free solid solutions, J. Phys. Condens. Matter. **16**, (2004), 963-70.

[17] *X. G. Tang, K. H. Chew*, H. L. W. Chan, Diffuse phase transition and dielectric tunability of $Ba(Zr_yTi_{1-y})O_3$ relaxor ferroelectric ceramics, Acta Mater. **52**, (2004), 5177-83.

[18] *R. Farhi, M. El Marssi, A. Simon, J. Ravez*, A Raman and dielectric study of ferroelectric $Ba(Ti_{1-x}Zr_x)O_3$ ceramics, Eur. Phys. J. B **9**, (1999), 599-604.

[19] *M. Deluca, C. A. Vasilescu, A. C. Ianculescu, D. C. Berger, C. E. Ciomaga, L. P. Curecheriu, L. Stoleriu, A. Gajovic, L. Mitoseriu, C. Galassi*, Investigation of the composition-dependent properties of $BaTi_{1-x}Zr_xO_3$ ceramics prepared by the modified Pechini method, J. Eur. Ceram. Soc. **32**, (2012), 3551–3566.

[20] *J. Bera, S. K. Rout*, On the formation mechanism of $BaTiO_3$ –$BaZrO_3$ solid solution through solid-oxide reaction, Mater. Lett. **59**, (2005), 135-138.

[21] *I. A. Santos, J. A. Eiras*, Phenomenological description of the diffuse phase transition in ferroelectrics, J. Phys. Condens. Matter. **13**, (2001), 11733-11740.

[22] *C. Ciomaga, M. Viviani, M.T. Buscaglia, V. Buscaglia, L. Mitoseriu, A. Stancu and P. Nanni*, Preparation and characterisation of the $Ba(Zr,Ti)O_3$ ceramics with relaxor properties, J. Eur. Ceram. Soc. **27**, (2007), 4061-4064.

[23] *D. Ricinschi, C.E. Ciomaga, L. Mitoseriu, V. Buscaglia and M. Okuyama*, erroelectric–relaxor crossover characteristics in $Ba(Zr_xTi_{1-x})O_3$ ceramics investigated by AFM-piezoresponse study, J. Eur. Ceram. Soc. **30**, (2010), 237-241.

[24] *L. Mitoseriu, A. Stancu, C. Fedor and P.M. Vilarinho*, Analysis of the composition-induced transition from relaxor to ferroelectric state in $Pb(Fe_{2/3}W_{1/3})O_3$ - $PbTiO_3$ solid solutions, J. Appl. Phys. **94**, (2003), 1918-1925.

[25] *A. K. Tagantsev, J. Lu, S. Stemmer*, Temperature dependence of the dielectric tunability of pyrochlore bismuth zinc niobate thin films, Appl. Phys. Lett. **86**, (2005), 032901 (1-3).

[26] *U. Bianchi, J. Dec, W. Kleemann, J. G. Bednorz*, Cluster and domain-state dynamics of ferroelectric $Sr_{1-x}Ca_xTiO_3$ ($x = 0.007$)**,** Phys. Rev. B **51**, (1995), 8737-8746.

[27] *N. Horchidan, A. C. Ianculescu, L. P. Curecheriu, F. Tudorache, V. Musteata, S. Stoleriu, N. Drăgan, D. Crişan, S. Tascu, L Mitoşeriu*, Preparation and characterization of barium titanate stannate solid solutions, J. Alloy Compd. **509**, (2011), 4731-4737.